

Topological Arrest of Ballooning Modes in Non-Axisymmetric Toroidal Plasmas

Amitava Bhattacharjee

Department of Astrophysical Sciences
Princeton University, Princeton, NJ 08540, USA*

(Dated: February 10, 2026)

Nonlinear ballooning instabilities in non-axisymmetric equilibria exhibit spatial localization along field lines that mirrors Anderson localization in disordered lattices. We demonstrate that this localization fundamentally alters nonlinear stability, transforming a global ballooning crash into a connectivity phase transition on a Ginzburg-Landau network. We identify a dimensionless number, denoted by η_c , as a topological threshold derived from continuum percolation theory. Below this threshold, global instability is topologically arrested as isolated scintillations, providing a rigorous explanation for the robust, benign saturation observed in experiments. Above this threshold, a spanning cluster path forms, unlocking rapid and potentially disruptive nonlinear growth.

I. INTRODUCTION

The pursuit of high-pressure plasma confinement in toroidal devices is often constrained by the threat of explosive ballooning crashes. However, a puzzling issue has emerged between theory and experimental reality: while axisymmetric tokamaks undergo catastrophic disruptions [1], highly non-axisymmetric stellarators such as LHD [2] and W7-X [3] operate safely within linearly unstable regimes.

Ballooning modes are typically characterized by long-wavelength structures aligned with field lines and short-wavelength structures perpendicular to them. Cuthbert and Dewar [4] showed that, in general toroidal geometry, ballooning eigenfunctions are exponentially localized along field lines and interpreted this behavior in terms of Anderson localization, a well-known phenomenon in condensed matter physics [5]. Redi et al. subsequently demonstrated that stellarator ballooning spectra exhibit signatures of quantum chaos [6]. These results suggest that three-dimensional (3D) geometry fundamentally alters the structure of ballooning modes. In this Letter, we show that Anderson localization converts weakly nonlinear ballooning dynamics into a Ginzburg-Landau system on a sparse network of localized structures. Nonlinear stability of ballooning modes is then governed by the connectivity of this network on a flux surface. We show that this resilience can be understood from a topological perspective. By mapping the flux surface onto a network of localized modes, we prove that global instability can be avoided unless the packet density and interaction radius exceed the percolation threshold of $\eta_c = 1.128$ [7]. This finding suggests that magnetic aperiodicity serves as a ‘topological safety net’ that preserves the integrity of the flux surface even under high pressure drive.

II. ANDERSON LOCALIZATION

In the high-toroidal-mode number limit, the linearized ballooning equation can be written as given by Cuthbert and Dewar [4, 8]:

$$\frac{d}{d\theta} \left[A(\theta) \frac{d\xi}{d\theta} \right] - [K(\theta) + \lambda N(\theta)] \xi = 0, \quad (1)$$

where ξ is related to the normal component of the plasma displacement, the coefficients $A(\theta)$, $K(\theta)$, and $N(\theta)$ are functions of the coordinate θ along a field line, and λ is the linear eigenfrequency squared. Because $A > 0$, this Sturm-Liouville problem can be transformed into the Schrödinger form

$$\left[\frac{d^2}{d\theta^2} + E - V(\theta) \right] y = 0, \quad (2)$$

where $y(\theta) = A^{1/2}(\theta) \xi(\theta)$. The effective potential depends on the equilibrium properties sampled along the field line. Our notation is identical to that of [4], and to save space, we do not reproduce the lengthy expressions for the various symbols here.

The essential distinction between axisymmetric and 3D toroidal geometry is the structure of the ballooning potential. In both cases, the potential contains a secular magnetic shear term that grows without bound as $|\theta| \rightarrow \infty$ and is not periodic. The crucial distinction lies instead in the behavior of the *geometric coefficients* that enter the ballooning equation. For axisymmetry, the curvature, metric coefficients, magnetic field strength, and pressure-gradient drive that enter the ballooning operator are periodic functions of the angle θ . As a field line winds around the torus, it samples the same geometric sequence repeatedly. The only nonperiodic contribution to the potential arises from the magnetic shear term, which confines the mode but does not introduce localization. As a result, the associated eigenfunctions are extended spatially and can be identified as Bloch solutions [4, 8]. In 3D geometry, by contrast, different field lines on the same flux surface sample different sequences of curvature and metric coefficients. Along a single field line, these

* amitava@princeton.edu

coefficients typically vary aperiodically as the line winds around the torus. This aperiodic geometric sampling, rather than the shear term, is what produces Anderson localization.

To see this, we discretize Eq. 2 on a uniform grid $\theta_n = n\Delta\theta$ and write it in transfer-matrix form

$$\begin{pmatrix} y_{n+1} \\ y_n \end{pmatrix} = T_n \begin{pmatrix} y_n \\ y_{n-1} \end{pmatrix}, \quad (3)$$

where T_n is the (2×2) transfer matrix determined by the local value of $V(\theta_n)$:

$$T_n = \begin{bmatrix} 2 + (\Delta\theta)^2 [V(\theta_n) - E] & -1 \\ 1 & 0 \end{bmatrix}. \quad (4)$$

The behavior of solutions for large $|n|$ is governed by the Lyapunov exponent [9]:

$$\gamma = \lim_{N \rightarrow \infty} \frac{1}{N} \|T_N T_{N-1} \cdots T_1\|. \quad (5)$$

Here, the vertical double bars denote any convenient matrix norm (e.g., the Frobenius norm), as the limiting value of γ is independent of the specific norm chosen. For 1D Schrödinger operators with aperiodic coefficients, products of transfer matrices generically have $\gamma > 0$, leading to exponentially localized states. This classical analytical result [5, 9] underlies Anderson localization and applies here because the geometric coefficients entering $V(\theta)$ vary aperiodically along a field line in 3D toroidal equilibria. A positive Lyapunov exponent implies exponential localization of eigenfunctions,

$$|y_n| \sim e^{-|n-n_0|/\ell} \quad (6)$$

where n_0 is the location of the localization center and $\ell \equiv \gamma^{-1}$ is the localization length. Cuthbert and Dewar [4] demonstrated the resulting exponential localization numerically. Note that Eq. 6 should be interpreted as smooth (upper bound) envelopes of the numerically calculated eigenfunctions by Cuthbert and Dewar, which exhibit significant fine structure within the envelopes.

III. THE GINZBURG-LANDAU NETWORK

To proceed further, we derive a time-dependent weakly nonlinear form of the ideal MHD equations by expanding the fully nonlinear ideal-MHD displacement equation in Lagrangian coordinates [10, 11]. In this formulation, the plasma position is written as $\mathbf{r}(\mathbf{r}_0, t) = \mathbf{r}_0 + \xi(\mathbf{r}_0, t)$, where ξ is the displacement from the initial position \mathbf{r}_0 . The exact ideal-MHD evolution equation for ξ contains various nonlinear terms. Expanding these quantities in powers of ξ produces a linear operator acting on ξ plus quadratic and higher-order nonlinear terms. The evolution equation for the normal component ξ , introduced in Eq. 1, has the schematic form

$$\partial_t \xi = \mathcal{L} \xi + \mathcal{N}_2(\xi, \xi) + \mathcal{N}_3(\xi, \xi, \xi). \quad (7)$$

Near marginal stability, nonlinear dynamics are governed by the weakly unstable eigenfunctions via standard center-manifold analysis [12]. Because these eigenfunctions are localized, the perturbation on this reduced manifold can be written as

$$\xi(\theta, t) = \sum_j a_j(t) \phi_j(\theta), \quad (8)$$

where $\phi_j(\theta)$ are the weakly unstable and localized eigenfunctions. Near marginal stability, we introduce a small parameter quantifying the system's deviation from marginal stability. As discussed in Appendix A, we obtain the Ginzburg-Landau equation as a normal form:

$$\dot{a}_j = \gamma_j a_j - \mu_j a_j^3 + \sum_{k \neq j} J_{jk} a_k, \quad (9)$$

where overlap integrals decay exponentially with separation

$$J_{jk} \sim J_0 e^{-d_{jk}/\ell}. \quad (10)$$

This is the discrete analogue of a Ginzburg-Landau equation defined on a network whose coupling is controlled by the localization length. (Note that in Eq. 9, γ_j is a linear growth rate, which should not be confused with the Lyapunov exponent, given by Eq. 5.)

Two localized structures interact effectively only if this coupling exceeds a characteristic dynamical scale J_* , thereby defining an effective interaction radius

$$R_* = \ell \ln \left(\frac{J_0}{J_*} \right). \quad (11)$$

On a flux surface, the centers θ_j of unstable localized packets are distributed with areal density $\rho(\beta)$, which increases as the pressure gradient exceeds the marginal value. The set of packets and their interaction radii, therefore, defines a random geometric graph on the flux surface. A standard result is that such a graph develops a surface-spanning connected cluster when the dimensionless parameter

$$\eta(\beta) = \rho(\beta) \pi R_*^2(\beta), \quad (12)$$

exceeds a critical value $\eta_c = \rho \pi R_*^2 = 1.128$, given by percolation theory [7], which can be tested in experiments as well as numerical simulations. Recent M3D-C1 simulations show regimes of benign saturation and crash-like behavior [13, 14]. In the present framework, these behaviors correspond naturally to subcritical and supercritical connectivity of localized ballooning structures, illustrated in Fig. 1.

To connect the percolation control parameter $\eta = \rho \pi R_*^2$ with experiment, we use published spatial statistics of edge fluctuations as proxies for the quantities entering this definition. In tokamaks, heterodyne reflectometry and beam emission spectroscopy measurements during the inter-ELM phase report radial correlation lengths

of density fluctuations on the order of 0.5–1 cm, which we take as a conservative estimate of the interaction radius R_* in that regime [15–17]. In contrast, fast imaging and probe measurements in stellarators such as W7-X and LHD [18, 19] show filamentary structures with shorter effective spatial scales and lower apparent areal density. Using these published spatial scales as proxies for structure size and interaction reach yields effective values of η that lie either below (for W7-X) or nearly at (for LHD) the continuum percolation threshold. Under inter-ELM conditions, DIII-D seems to lie in a moderately supercritical regime. When DIII-D exhibits a global ELM crash, we crudely estimate that the plasma would be supercritical with η exceeding 20.

We emphasize that the values shown in Fig. 2 are schematic: no published study directly reports the event density ρ or the interaction radius R_* in the percolation sense. A quantitative experimental determination of η would require dedicated analysis of spatiotemporal diagnostics. Such an analysis would (i) identify coherent fluctuation structures in imaging or probe data, (ii) measure $\rho = N/A$ from event counts in a fixed observation region, and (iii) determine R_* from conditional spatial-temporal correlation functions of these events. This program would convert Fig. 2 from a schematic regime map into a fully data-driven experimental test of the theory. W7-X appears to be in the subcritical regime even at high pressure, demonstrating that 3D geometric disorder provides a topological safety net against global ballooning collapses. It seems to possess sufficient symmetry-breaking to shred ballooning modes into isolated filamentary scintillations, with enough symmetry for good confinement, yet enough disorder to prevent profile-terminating disruptions.

IV. CONCLUSIONS

In conclusion, we have demonstrated that 3D geometry converts ballooning dynamics from a single global mode into a Ginzburg–Landau system on a network of Anderson-localized states. Nonlinear stability is therefore a connectivity property of this network. The Anderson mechanism is lost in the case of pure axisymmetry. In the presence of some form of symmetry-breaking, such as that imposed by resonant magnetic perturbations in a tokamak, ballooning modes can be suppressed.

Recent work suggests that in quasisymmetric equilibria the magnetic field strength along a flux surface may possess an underlying structure associated with integrable systems such as the KdV equation [20]. If so, the ballooning potential in quasisymmetric stellarators may not belong to the aperiodic class responsible for Anderson localization. While Anderson localization provides a natural explanation for benign nonlinear scintillations (or more colloquially, fizz) in generic 3D equilibria, stellarators with perfect quasisymmetry may prove to be as vulnerable to nonlinear ballooning modes as axisymmetric

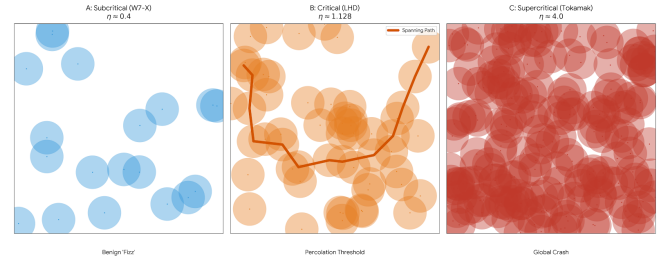


FIG. 1. Topological connectivity of ballooning modes on a toroidal flux surface. The spatial distribution and interaction of localized ballooning mode structures are shown for three characteristic magnetic geometries. Each circle represents the interaction radius of a mode. (a) Subcritical regime (W7-X): High magnetic aperiodicity (large Lyapunov exponent) leads to short localization lengths. The resulting connectivity parameter η is well below η_c , preventing global synchronization and resulting in benign topological arrest. (b) Critical Regime (LHD): Reduced geometric disorder increases the interaction radius, bringing the system to the marginal percolation threshold ($\eta_c = 1.128$). In this regime, a global-spanning path (orange line) intermittently forms, thereby facilitating the bursty MHD activity observed experimentally. (c) Supercritical Regime (DIII-D): Near-perfect axisymmetry leads to effectively infinite localization lengths. The system is in a highly connected state, where global phase-locking of modes enables the explosive, singular growth characteristic of major profile crashes.

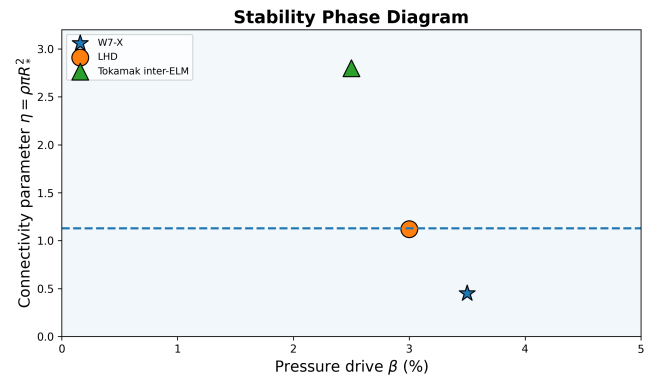


FIG. 2. Schematic estimates of the connectivity parameter $\eta = \rho \pi R_*^2$ for representative operating regimes. The dashed line indicates the continuum percolation threshold $\eta_c \simeq 1.13$. The tokamak point is based on measured inter-ELM radial correlation lengths of edge density fluctuations obtained from reflectometry and BES diagnostics [15–17]. The stellarator points reflect shorter spatial scales associated with filamentary structures observed in W7-X and LHD [18, 19]. These values are *not* direct extractions of ρ and R_* from experimental event statistics but proxy estimates based on published spatial scales, intended to illustrate the separation of regimes. A program for quantitative determination of ρ and R_* from spatiotemporal diagnostics is described in the text.

tokamaks. By strategically retaining a degree of geometric aperiodicity, we can design reactors that are topologically immune to global ballooning crashes, trading near-perfect quasisymmetry for nonlinear stability.

We would like to thank A. Brown, S. Buller, and W. Sengupta for helpful discussions. We acknowledge the use of ChatGPT and Gemini (Google) large language models for assistance with drafting, making figures, organizing ideas, and navigating the literature. This research was supported by a grant from the Simons Foundation/SFARI (560651, AB) and the Department of Energy (DOE) Award No. DE-SC0024548 (until March 31, 2025). We are grateful to Princeton University for generously supporting our research during the suspension period of our DOE Award.

Appendix A: Derivation of the Ginzburg-Landau Equation for Ballooning

We describe how the weakly nonlinear Ginzburg-Landau-type evolution follows from the fully nonlinear Lagrangian ideal-MHD displacement equation. Let $\xi(\mathbf{a}, t)$ denote the Lagrangian displacement of a fluid element labeled by \mathbf{a} . In Lagrangian variables, ideal MHD admits an exact equation of motion of the form [10, 11]

$$\rho_0(\mathbf{a})\partial_t^2\xi = \mathcal{F}[\xi], \quad (\text{A1})$$

where $\mathcal{F}[\xi]$ is a nonlinear force functional arising from magnetic and pressure stresses expressed through the deformation of the equilibrium configuration. Expanding about equilibrium $\xi = 0$ gives

$$\mathcal{F}[\xi] = \mathcal{L}\xi + \mathcal{Q}(\xi, \xi) + \mathcal{C}(\xi, \xi, \xi) + \dots, \quad (\text{A2})$$

where \mathcal{L} is the linear ideal-MHD force operator and \mathcal{Q} , \mathcal{C} are quadratic and cubic nonlinearities. We introduce the velocity $\mathbf{v} = \partial_t\xi$. Equation A1 is equivalent to the first-order system

$$\partial_t \begin{pmatrix} \xi \\ \mathbf{v} \end{pmatrix} = \begin{pmatrix} 0 & I \\ \rho_0^{-1}\mathcal{L} & 0 \end{pmatrix} \begin{pmatrix} \xi \\ \mathbf{v} \end{pmatrix} + \mathbb{N}_2 + \mathbb{N}_3 + \dots, \quad (\text{A3})$$

where \mathbb{N}_2 , \mathbb{N}_3 arise from \mathcal{Q} , \mathcal{C} . This step is exact and involves no approximation.

Near marginal ballooning stability the spectrum of \mathcal{L} contains a finite set of weakly unstable (or weakly

damped) eigenvalues separated from fast Alfvénic modes. Under this (standard) hypothesis, the dynamics admits a finite-dimensional center (or center-unstable) manifold parameterized by amplitudes $a_j(t)$ associated with these eigenvectors. Representing the displacement by its normal component along a field line, denoted $\xi(\theta, t)$, it can be shown after some algebra that the slow-manifold evolution may be written schematically as

$$\partial_t\xi = \mathcal{L}\xi + \mathcal{N}_2(\xi, \xi) + \mathcal{N}_3(\xi, \xi, \xi) + \dots. \quad (\text{A4})$$

Let $\phi_j(t)$ denote the eigenfunctions of the linear ballooning operator,

$$\mathcal{L}\phi_j = \gamma_j\phi_j, \quad (\text{A5})$$

and expand the displacement on the slow manifold as

$$\xi(\theta, t) = \sum_j a_j(t)\phi_j(\theta). \quad (\text{A6})$$

Substituting Eq. A6 into Eq. A4, differentiating in time, and projecting onto the adjoint eigenfunctions ϕ_j^\dagger yields the amplitude equations

$$\dot{a}_j = \gamma_j a_j + \sum_{kl} c_{j;kl}^{(2)} a_k a_l + \sum_{klm} c_{j;klm}^{(3)} a_k a_l a_m + \dots \quad (\text{A7})$$

about equilibrium. In the axisymmetric case, it can be shown that the 3D geometric noise “shreds” the phase-sensitive quadratic drive into zero, reducing the system from an explosive regime to a saturated Ginzburg-Landau regime dominated by local cubic damping. This vanishing of the quadratic coupling is a topological consequence of Anderson localization in the 3D aperiodic field, which introduces decoherence among the localized wavepackets, forcing the nonlinear evolution into a cubic Ginzburg-Landau regime, where stability is governed solely by the connectivity of the localized packets. Retaining the leading contributions gives

$$\dot{a}_j = \gamma_j a_j - \mu_j a_j^3 + \sum_{k \neq j} J_{jk} a_k, \quad (\text{A8})$$

with $J_{jk} \sim e^{-d_{jk}/\ell}$. This is a discrete Ginzburg-Landau (Stuart-Landau) network, which is the form used in the main text.

[1] E. Strait, Physics of Plasmas **1**, 1415 (1994).
[2] H. Yamada et al, Fusion Science and Technology **51**, 12 (2010).
[3] O. Grulke et al, Nuclear Fusion **64**, 11202 (2024).
[4] P. Cuthbert and R. L. Dewar, Physics of Plasmas **7**, 2302 (2000).
[5] P. W. Anderson, Absence of diffusion in certain random lattices, Physical Review **109**, 1492 (1958).
[6] M. H. Redi et al, Anderson localization of ballooning modes, quantum chaos and the stability of compact quasiazimuthally symmetric stellarators, Physics of Plasmas **9**, 1990 (2002).

- [7] J. Quintanilla, S. Torquato, and R. M. Ziff, *Journal of Physics A: Mathematical and General* **33**, L399 (2000).
- [8] R. L. Dewar and A. H. Glasser, *Physics of Fluids* **26**, 3038 (1983).
- [9] A. Crisanti, G. Paladin, and A. Vulpiani, *Products of Random Matrices in Statistical Physics* (Springer-Verlag, 1993).
- [10] S. C. Cowley and M. Artun, *Physics Reports* **283**, 185 (1997).
- [11] P. Zhu and C. C. Hegna, *Physics of Plasmas* **15**, 092306 (2008).
- [12] J. D. Crawford, *Rev. Mod. Phys.* **63**, 991 (1991).
- [13] A. M. Wright and N. M. Ferraro, *Physics of Plasmas* **31**, 082509 (2024).
- [14] Y. Zhou et al, *Phys. Rev. Lett.* **133**, 135102 (2024).
- [15] Z. Yan et al, *Physics of Plasmas* **18**, 056117 (2011).
- [16] T. L. Rhodes, R. J. Taylor, and W. A. Peebles, *Review of Scientific Instruments* **66**, 824 (1995).
- [17] K. Barada et al, *Nuclear Fusion* **61**, 126037 (2021).
- [18] A. Buzas et al, *Nuclear Fusion* **64**, 066012 (2020).
- [19] K. Tanaka et al, *Plasma and Fusion Research* **7**, 1402152 (2012).
- [20] W. Sengupta et al, *Physics of Plasmas* **32**, 102509 (2025).